STAR Protocols

CellPress
OPEN ACCESS

Protocol

Rational engineering enables co-crystallization and structural determination of the HIV-1 matrix-tRNA complex

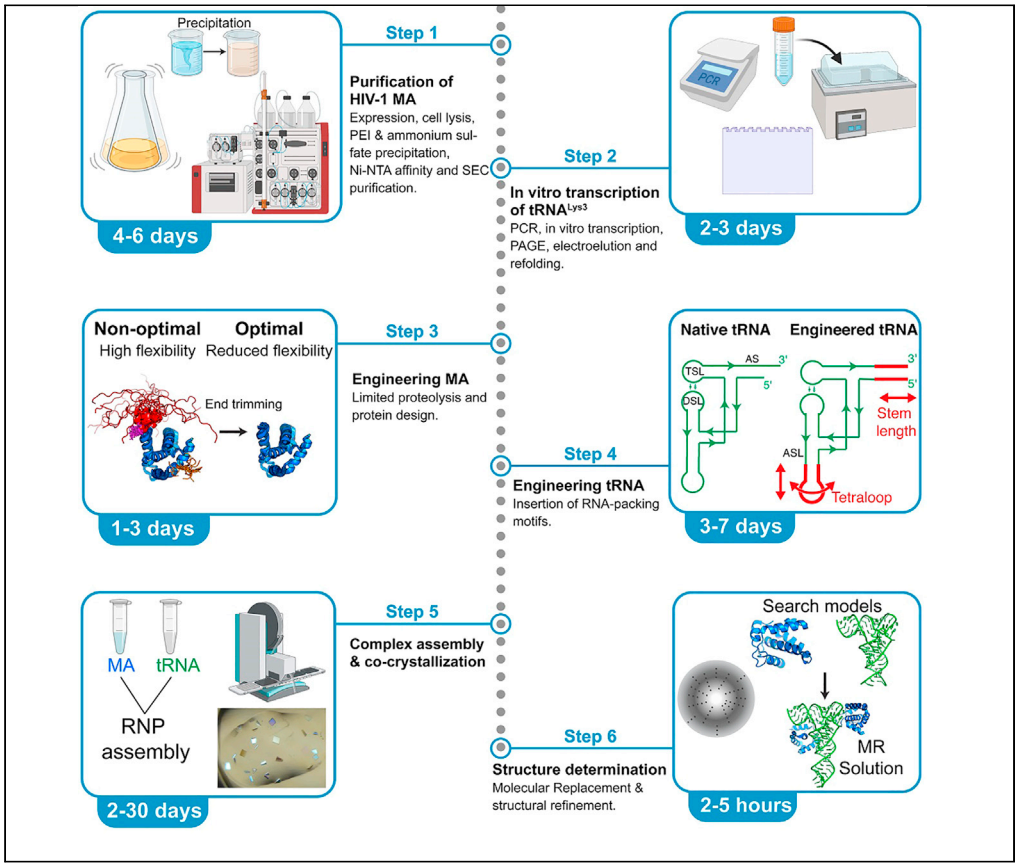

Host tRNAs specifically interact with the matrix domain (MA) of HIV-1 major structural polyprotein, Gag, to control its membrane localization and virion assembly. In this protocol, we describe the purification and engineering of HIV-1 MA and tRNA, and the co-crystallization and structure determination of the complex using X-ray crystallography. Rational engineering of the tRNA surface created tRNA-tRNA packing contacts that drove the formation of diffraction-quality co-crystals. This protocol can be adapted to solve other ribonucleoprotein complex structures containing structured RNAs.

Charles Bou-Nader, Jinwei Zhang

charles.bou-nader@nih.gov (C.B.-N.)
jinwei.zhang@nih.gov (J.Z.)

Highlights

Protocol to purify HIV-1 matrix domain and to transcribe human tRNA^{Lys3} in high yields

Use of limited proteolysis to engineer HIV-1 MA protein for co-crystallization

Rational tRNA engineering to promote RNA-RNA contacts for co-crystallization

Details for crystallization of MA-tRNA complex and steps for structural determination

Bou-Nader & Zhang, STAR Protocols 3, 101056
March 18, 2022
https://doi.org/10.1016/j.xpro.2021.101056

STAR Protocols

CellPress
OPEN ACCESS

Protocol

Rational engineering enables co-crystallization and structural determination of the HIV-1 matrix-tRNA complex

Charles Bou-Nader[1,2,*] and Jinwei Zhang[1,3,*]

[1]Laboratory of Molecular Biology, National Institute of Diabetes and Digestive and Kidney Diseases, Bethesda, MD 20892, USA

[2]Technical contact

[3]Lead contact

*Correspondence: charles.bou-nader@nih.gov (C.B.-N.), jinwei.zhang@nih.gov (J.Z.)
https://doi.org/10.1016/j.xpro.2021.101056

SUMMARY

Host tRNAs specifically interact with the matrix domain (MA) of HIV-1 major structural polyprotein, Gag, to control its membrane localization and virion assembly. In this protocol, we describe the purification and engineering of HIV-1 MA and tRNA, and the co-crystallization and structure determination of the complex using X-ray crystallography. Rational engineering of the tRNA surface created tRNA-tRNA packing contacts that drove the formation of diffraction-quality co-crystals. This protocol can be adapted to solve other ribonucleoprotein complex structures containing structured RNAs.

For complete details on the use and execution of this protocol, please refer to Bou-Nader et al. (2021).

BEFORE YOU BEGIN

The protocol below describes the detailed steps for the structural characterization of the HIV-1 matrix protein (MA)-tRNA^{Lys3} complex. First, we describe the expression and purification of MA and the identification of a minimal protein domain that promotes crystallization. Second, we describe the in vitro transcription and purification of human tRNA^{Lys3} and its rational engineering with RNA motifs known to promote the formation of stable crystal-packing contacts. We then describe the in vitro reconstitution and isolation of the ribonucleoprotein complex, its crystallization and structure determination by molecular replacement.

KEY RESOURCES TABLE

REAGENT or RESOURCE	SOURCE	IDENTIFIER
Bacterial and virus strains		
BL21-CodonPlus (DE3)-RIL Competent Cells	Agilent	Cat# 230245
Critical commercial assays		
QuikChange Lightning	Agilent	Cat#210519
Deposited data		
Atomic coordinates and structure factor amplitudes for the co-crystal structure of HIV-1 MA bound to human tRNA^{Lys3}	(Bou-Nader et al., 2021)	PDB: 7MRL

(*Continued on next page*)

Continued

REAGENT or RESOURCE	SOURCE	IDENTIFIER
Oligonucleotides		
Forward primer to in vitro transcribed $tRNA^{Lys3}$ 5′-GGAATTCCTAATACGACTCACTATAGCC CGGATAGCTCAGTCGGT-3′	Integrated DNA Technologies	N/A
Reverse primer to in vitro transcribed $tRNA^{Lys3}$ 5′-UmGmGCGCCCGAACAGGGACTTGAA CCC-3′	Integrated DNA Technologies	N/A
Reverse primer to in vitro transcribed $tRNA^{Lys3}$ used to solve final co-crystal structure 5′-AmCmCCGAACAGGGACTTGAAC-3′	Integrated DNA Technologies	N/A
Forward primer to in vitro transcribed $tRNA^{Lys3}$ used to solve final co-crystal structure 5′-GGAATTCCTAATACGACT CACTATAGGGAGAGCTATCCGGGT CTGATGAGTCCGTGAGGACGAAA CGGTACCCGGTACCGTCACCCGG ATAGCTCAGTCG-3′	Integrated DNA Technologies	N/A
Recombinant DNA		
pET19b-MA	(Gaines et al., 2018)	N/A
Software and algorithms		
SEDPHAT	(Zhao et al., 2015)	RRID:SCR_016254 http://www.analyticalultracentrifugation.com/sedphat/
NITPIC	(Keller et al., 2012)	https://www.utsouthwestern.edu/labs/mbr/software/
SEDFIT	(Schuck, 2000)	RRID:SCR_018365 https://sedfitsedphat.nibib.nih.gov/software/default.aspx
REDATE	(Zhao et al., 2013)	https://www.utsouthwestern.edu/labs/mbr/software/
SEDNTERP	(Cole et al., 2008)	RRID:SCR_016253 http://www.jphilo.mailway.com/sednterp.htm
ASTRA	Wyatt Technology Europe	RRID:SCR_016255 https://www.wyatt.com/products/software/astra.html
Phaser	(McCoy et al., 2007)	RRID:SCR_014219 https://www.phenix-online.org/documentation/reference/phaser.html
Phenix	(Liebschner et al., 2019)	RRID:SCR_014224 https://www.phenix-online.org
Coot	(Emsley et al., 2010)	RRID:SCR_014222 https://www2.mrc-lmb.cam.ac.uk/personal/pemsley/coot/
ERRASER	(Chou et al., 2013)	https://rosie.graylab.jhu.edu/erraser
Other		
Origin	OriginLab Corporation	RRID:SCR_014212 https://www.originlab.com/

MATERIALS AND EQUIPMENT

Lysis Buffer

Reagent	Final concentration	Amount
Tris-HCl pH 7.5 (1 M)	25 mM	25 mL
NaCl (5 M)	200 mM	40 mL
Glycerol (100% v/v)	5% v/v	50 mL
β-mercaptoethanol (14 M)	10 mM	0.7 mL
ddH_2O	n/a	884.3 mL
Total	**n/a**	**1 L**

Store at 4°C for 1 week.

Add one tablet of SIGMAFAST protease inhibitor in the cell resuspension.

PEI stock		
Reagent	Final concentration	Amount
Poly(ethyleneimine) (50% w/v)	15% w/v	150 mL
ddH_2O	n/a	350 mL
Total	**n/a**	**500 mL**
Adjust pH to ~7 using HCl.		
Store at 25°C or 4°C for ~6 months.		

HisTrap Loading Buffer		
Reagent	Final concentration	Amount
Tris-HCl pH 7.5 (1 M)	25 mM	25 mL
NaCl (5 M)	500 mM	100 mL
Glycerol (100% v/v)	10% v/v	100 mL
Imidazole	15 mM	1.02 g
β-mercaptoethanol (14 M)	10 mM	0.7 mL
ddH_2O	n/a	774.3 mL
Total	**n/a**	**1 L**
Store at 4°C for 1 week.		

HisTrap Elution Buffer		
Reagent	Final concentration	Amount
Tris-HCl pH 7.5 (1 M)	25 mM	25 mL
NaCl (5 M)	500 mM	100 mL
Glycerol (100% v/v)	10% v/v	100 mL
Imidazole	250 mM	17.02 g
β-mercaptoethanol (14 M)	10 mM	0.7 mL
ddH_2O	n/a	774.3 mL
Total	**n/a**	**1 L**
Store at 4°C for 1 week.		

Gel Filtration Buffer		
Reagent	Final concentration	Amount
Tris-HCl pH 7.5 (1 M)	25 mM	25 mL
NaCl (5 M)	150 mL	30 mL
$MgCl_2$ (1 M)	2 mM	2 mL
DEPC H_2O (RNase-free)	n/a	943 mL
Total	**n/a**	**1 L**
Store at 4°C indefinitely.		

10× T7 transcription buffer		
Reagent	Final concentration	Amount
Triton X-100 (1% v/v)	0.1% (v/v)	5 mL
Spermidine (1 M)	20 mM	1 mL
DTT (1 M)	100 mM	5 mL
Tris-HCl pH 8.1 (2 M)	300 mM	7.5 mL
$MgCl_2$ (1 M)	250 mM	12.5 mL
DEPC H_2O (RNase-free)	n/a	19 mL
Total	**n/a**	**50 mL**
Store at −20°C indefinitely.		

10× TBE		
Reagent	Final concentration	Amount
Tris Base	0.892 M	432 g
Boric Acid	0.889 M	220 g
EDTA (0.5 M)	20 mM	160 mL
DEPC H_2O (RNase-free)	n/a	~3.3 L
Total	**n/a**	**4 L**
Store at 25°C indefinitely.		

2× Denaturing gel loading buffer		
Reagent	Final concentration	Amount
Formamide (100% v/v)	95% v/v	47.5 mL
SDS (10% w/v)	0.025% w/v	125 µL
Bromophenol Blue	0.025% w/v	12.5 mg
Xylene Cyanol	0.025% w/v	12.5 mg
EDTA (0.5 M)	1 mM	100 µL
DEPC H_2O (RNase-free)	n/a	2.275 mL
Total	**n/a**	**50 mL**
Store at 4°C or −20°C indefinitely.		

10× THE buffer		
Reagent	Final concentration	Amount
Tris Base	0.165 M	40 g
HEPES	0.329 M	157 g
EDTA (0.5 M)	0.5 mM	2 mL
DEPC H_2O (RNase-free)	n/a	~1.8 L
Total	**n/a**	**2 L**
Store at 25°C indefinitely.		

2× Non-denaturing gel loading buffer		
Reagent	Final concentration	Amount
Tris-HCl pH 7 (1 M)	100 mM	5 mL
Glycerol (100% v/v)	20% w/v	10 mL
Bromophenol Blue	0.025% w/v	12.5 mg
Xylene Cyanol	0.025% w/v	12.5 mg
DEPC H_2O (RNase-free)	n/a	35 mL
Total	**n/a**	**50 mL**
Store at 4°C or −20°C indefinitely.		

4× SDS gel loading buffer		
Reagent	Final concentration	Amount
Tris-HCl pH 7 (1 M)	62.5 mM	3.125 mL
Glycerol (100% v/v)	10% w/v	5 mL
Bromophenol Blue	0.025% w/v	12.5 mg
DTT (1 M)	10 mM	0.5 mL
SDS (10% w/v)	2.5% w/v	12.5 mL
DEPC H_2O (RNase-free)	n/a	28.875 mL
Total	**n/a**	**50 mL**
Store at 4°C or −20°C indefinitely.		

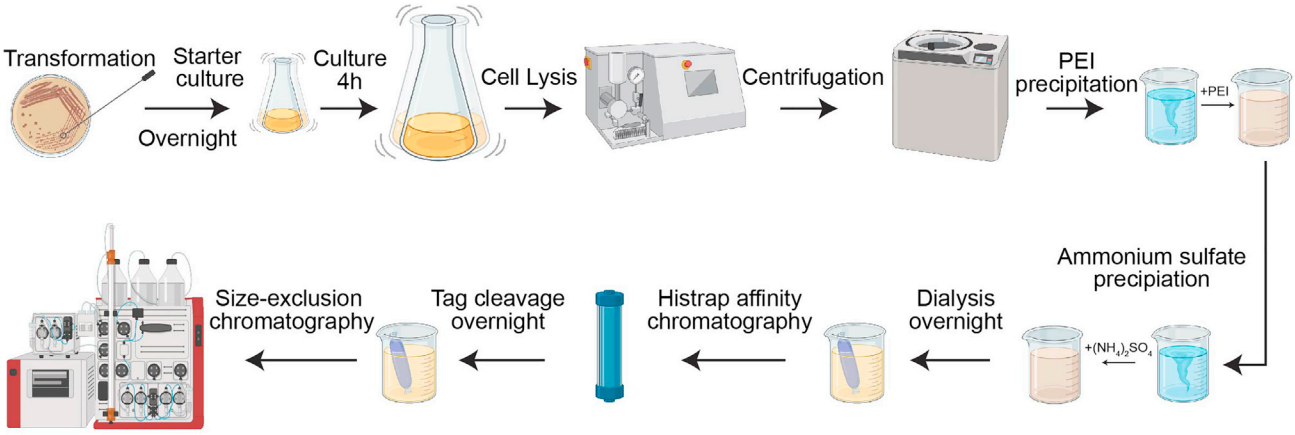

Figure 1. Workflow for purification of HIV-1 Gag matrix domain

⚠ CRITICAL: β-mercaptoethanol and Sodium dodecyl sulfate (SDS) powders are toxic and thus should always be handled with gloves under a hood while avoiding any direct contact with the chemical.

STEP-BY-STEP METHOD DETAILS

Purification of the HIV-1 matrix domain

Timing: 4–6 days

1. Transformation: Transform 40 μL of BL21(DE3)-RIL cells with 1 μL of pET19b vector (~100 ng/μL) containing an N-terminally his-tagged HIV-1 matrix domain gene (Gaines et al., 2018). Spread 100 μL of cells onto an LB agar plate containing 100 μg/mL ampicillin and incubate it at 37°C for 16 h (Figure 1).

⚠ CRITICAL: This approach will yield unmyristoylated HIV-1 MA protein. To obtain myristoylated MA, transformation should be performed with a vector that expresses both HIV-1 MA and yeast N-myristoyltransferase (Tang et al., 2004).

2. Preculture: Transfer a single colony from the LB agar plate to a flask containing 100 mL of LB with 100 μg/mL of ampicillin and 25 μg/mL of chloramphenicol (required to maintain the pACYC-based plasmid containing extra copies of rare tRNAs in BL21(DE3)-RIL cells). Incubate this initial culture for 16 h at 37°C in a shaker at 200 rpm.
3. Cell culture and induction: Measure the optical density at 600 nm (OD_{600}) of the pre-culture. The value should be ~2. Inoculate 1 L LB media supplemented with 100 μg/mL of ampicillin and 25 μg/mL of chloramphenicol, with the pre-culture at a ratio of 1:80 and incubate at 37°C in a shaker at 200 rpm. Monitor the OD_{600} until it reaches ~0.6 then induce with 1 mM of isopropyl 1-thio-β-D-galactopyranoside (IPTG) and grow the cells for an additional 4 h at 37°C.
4. Cell harvesting: Measure the OD_{600} of the cultures (value should be ~1.8) and harvest the cells by centrifugation for 10 min at 4°C and ~5,400 g.

Pause point: Cell pellets can be resuspended in a lysis buffer following centrifugation and stored at −80°C until further purification.

5. Cell lysis and clarification: Resuspend cell pellets using 20 mL of lysis buffer per 1 L of LB culture. Lyse the cells either by sonication using a larger flat tip (0.25–1.0 inch diameter) or using a M110P or similar microfluidizer.

a. Centrifuge the lysed mixture for 45 min at 96,000 g at 4°C.
b. Recover the clarified supernatant and discard the pellet.

6. Polyethylenimine (PEI) precipitation: Add dropwise from a PEI stock (15% w/v) to the clarified supernatant to reach a final concentration of 0.15% w/v PEI at 4°C while stirring. For a total volume of 100 mL of supernatant add a total volume of 1 mL of PEI 15% w/v.

Note: Following the addition of PEI to the lysed supernatant, a strong white precipitation should occur.

a. Stir for an additional 30 min at 4°C.
b. Centrifuge at ~61,000 g at 4°C for 30 min.
c. Recover the supernatant and discard the white pellet.

Note: For most nucleic-acid-binding proteins, it is generally necessary to first identify a suitable PEI concentration and precipitation protocol appropriate for the specific protein (Burgess, 2009). In addition, the PEI stock has a basic pH >9. Although not necessary for MA purification, it is best to adjust its pH using HCl to near neutral for general usage.

Note: Performing the PEI and the ammonium sulfate precipitations is necessary to avoid nucleic acid and RNase contamination of the purified MA protein.

7. Ammonium sulfate precipitation: To remove the PEI and recover the protein from the supernatant, precipitate most proteins by slowly adding ammonium sulfate powder at 4°C while stirring until 90% saturation. For every 100 mL of supernatant at 4°C, add approximately 62.14 g of ammonium sulfate powder to achieve 90% saturation.

Note: Different proteins precipitate at different concentrations of ammonium sulfate due to different overall hydrophobicity and optimal concentrations should be empirically determined. Strong precipitation should occur during the addition of ammonium sulfate to the supernatant. For problems that may arise during this step, please refer to troubleshooting problem 1 below.

a. Stir for an additional 2 h at 4°C.
b. Centrifuge at 32,000 g for 20 min at 4°C.
c. Discard the supernatant and recover the pellet.
d. Resuspend the pellet in HisTrap loading buffer.
e. Dialyze the resuspended pellet against a 60-fold volume of HisTrap loading buffer for 16 h at 4°C to reduce the ammonium sulfate content. Use a dialysis membrane with a molecular weight cutoff (MWCO) of 3 kDa.
f. Filter the dialyzed sample with 0.22 μm filters to remove particles and aggregates.

8. Ni-NTA affinity chromatography: This step can be performed using either a fast protein liquid chromatography (FPLC) system, or manually using gravity-flow on a slurry of Ni-NTA resin. Here we detail the steps using a prepacked HisTrap HP 5 mL column operated by an AKTA PURE system and experimenters should follow the manufacturer's instructions for column handling, washing and storage.
a. Load the filtered protein sample onto the HisTrap HP 5 mL, collect the flowthrough.
b. Wash the column with 20 column volumes (CV) of HisTrap loading buffer.
c. Elute the bound protein either using 6 CV of HisTrap elution buffer (containing 250 mM imidazole) in a single step or using a linear gradient from 0% to 100% of HisTrap elution buffer over 10 CV. Both approaches lead to the elution of HIV-1 MA from the HisTrap with similar purities.

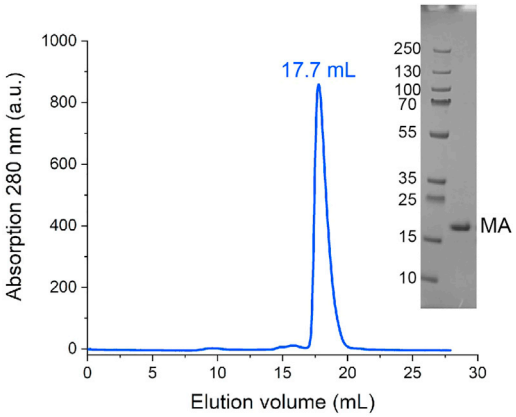

Figure 2. Size-exclusion chromatography (SEC) profile on a Superdex 200 Increase 10/300 GL column of freshly purified HIV-1 matrix protein (MA) and its purity analysis by SDS-PAGE

d. Run SDS-polyacrylamide gel electrophoresis (PAGE) to check the purity and pool fractions that contain the MA protein.

9. Cleavage of the his-tag: To remove the his-tag, the pooled MA protein is incubated with the TEV (Tobacco Etch Virus) protease at a molar ratio of 150:1 (MA:TEV), and the mixture is dialyzed 16 h against a 60-fold volume of Gel Filtration Buffer at 4°C.

Note: It is useful to identify optimal conditions for his-tag cleavage by testing different ratios of TEV protease and incubation time on a smaller scale.

10. Size-exclusion chromatography: Filter the dialyzed protein with 0.22 μm filters and measure the protein concentration using the absorption at 280 nm. Equilibrate the gel filtration column with the Gel Filtration Buffer. The size and amount of the protein will dictate which gel filtration column to use based on the manufacturer's instructions. When large amounts of proteins are present, use the HiLoad Superdex 200 16/600 as a final step for MA purification, or HiLoad Superdex 75 16/600 for slightly better separation. For analytical purposes, the Superdex 200/75 Increase 10/300 column can be used. Run SDS-PAGE to check the purity and pool fractions containing MA protein with sufficient purity (Figure 2). Store the purified protein at −80°C in small aliquots to avoid repeated cycles of freezing and thawing. The usual yield is ~0.8 mg purified MA per 1 L of LB culture.

In vitro transcription of human $tRNA^{Lys3}$ by T7 RNA polymerase

Timing: 2–3 days

11. Design a vector containing the DNA sequence of human $tRNA^{Lys3}$: Order a vector containing the following tRNA gene sequence: GCCCGGATAGCTCAGTCGGTAGAGCATCAGACTTTTAATCTGAGGGTCCAGGGTTCAAGTCCCTGTTCGGGCGCCA.
12. Design primers to amplify DNA template: Instead of using restriction enzyme-linearized vector as templates for in vitro transcription, the following primers are used to amplify the DNA template by PCR, to achieve higher yield:
    a. Forward primer: 5′-GGAATTCCTAATACGACTCACTATAGCCCGGATAGCTCAGTCGGT-3′. Underlined is the T7 promoter sequence required to initiate transcription by the T7 RNA polymerase. Downstream of the T7 promoter sequence are the 20 nucleotides (nt) found at the 5′ of wild type human $tRNA^{Lys3}$. The T7 promoter sequence will not be included in the final RNA product.
    b. Reverse primer: 5′-UmGmGCGCCCGAACAGGGACTTGAACCC-3′. This sequence is the reverse complement of the 26 nucleotides found at the 3′ of wild type human $tRNA^{Lys3}$, including its GCCA overhang. Underlined are two 2′-O-methyl-modified nucleotides

required to reduce heterogeneities at the 3′ end of the RNA product due to nontemplated nucleotide addition activity of T7 RNA polymerase (RNAP) (Kao et al., 1999).

Note: A purine is required downstream of the T7 promoter sequence to achieve high yields by wild-type T7 RNAP. Higher yields of transcribed RNAs are obtained with GGG>GG>G>A at the +1 position.

⚠ CRITICAL: The homogeneity of RNAs is critical for successful crystallization. In the event that the approach described above leads to heterogeneous transcripts during in vitro transcription, alternative primers should be used, or use *cis*- or *trans*-cleaving ribozymes to provide clean ends (Ferré-D'Amaré and Doudna, 1996). Please refer to troubleshooting problem 2 below.

13. PCR amplification of DNA template: Perform a touchdown PCR by gradually reducing the annealing temperature following the conditions below (Figure 3A):
    a. Assemble the PCR reaction components using the manufacturer's instructions for *Taq* DNA Polymerase with standard *Taq* buffer from NEB .

Note: Other commercially available or in-house purified DNA polymerases can be used.

    b. Add 500 ng of plasmid containing the gene for the human $tRNA^{Lys3}$
    c. Add forward and reverse primers to the mixture to 5 μM each.

PCR cycling conditions

Steps	Temperature	Time	Cycles
Initial Denaturation	95°C	3 min	1
Denaturation	95°C	30 s	20 cycles
Annealing	60°C (−0.5°C increment per cycle)	30 s	
Extension	72°C	1 min	
Denaturation	95°C	30 s	1
Annealing	45°C	30 s	1
Final Extension	72°C	30 s	1
Hold	4°C	Forever	

14. Confirm the successful amplification of the DNA template by running a 1.5% agarose gel at 125 V for 20 min. This gel can be prepared by dissolving 1.5 g of agarose into 100 mL of 1× Tris-acetate-EDTA (TAE) buffer. Add ethidium bromide or SYBR Gold stain before the gel solidifies to visualize the DNA species using a gel imager.

⚠ CRITICAL: Ethidium bromide and SYBR Gold are potent mutagens and should always be handled with appropriate personal protection gear (i.e. gloves, safety glasses, and others).

15. Set up the in vitro transcription reaction: To obtain sufficient amounts of RNA required for structural characterization, prepare a 5 mL in vitro transcription reaction as below:
    a. To 2.25 mL of RNase-free water, add 1 mL of PCR product from step 13.
    b. Add 0.5 mM of 10× T7 transcription buffer.
    c. Add 0.25 mL of each nucleoside triphosphate (NTP) at 0.1 M (ATP, CTP, GTP and UTP) to reach a final concentration of 5 mM for each NTP.
    d. Add 0.1 mL of 1 M $MgCl_2$ to reach a final concentration of 20 mM $MgCl_2$ in the mixture.
    e. Add 0.15 mL of 1 mg/mL in-house purified T7 RNAP. Follow manufacturer's instructions if commercial T7 RNAP is used.
    f. Add 10 μL of 1 mg/mL pyrophosphatase

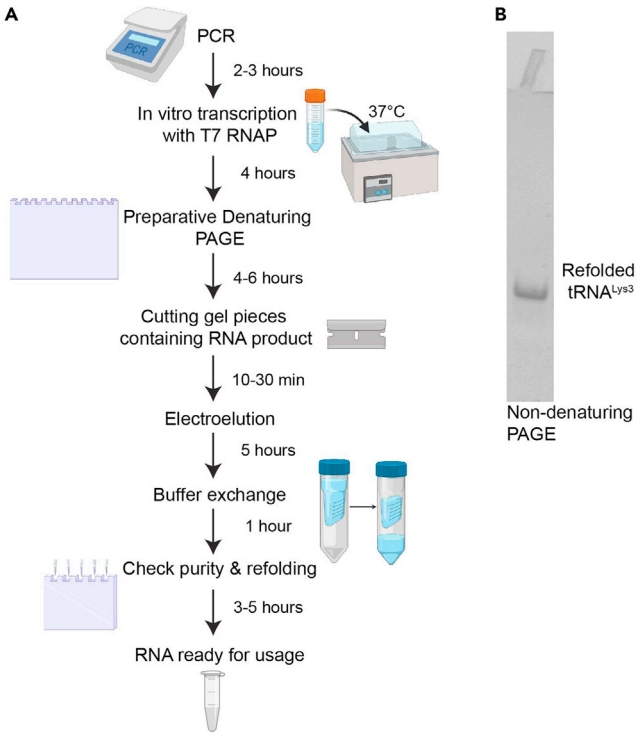

Figure 3. Preparation of $tRNA^{Lys3}$

(A) Workflow for preparation of in vitro transcribed RNA suitable for crystallization.

(B) Non-denaturing PAGE analysis of snap cooled $tRNA^{Lys3}$.

g. Incubate the final mixture in a water bath at 37°C for 4 h.

Note: Nuclease- and RNase-free water can be purchased from vendors. Alternatively, to inactivate RNases in Milli-Q water, add 1 mL of diethyl pyrocarbonate (DEPC) to 4 L of water and autoclave the solution for 1 hour to remove DEPC.

⚠ CRITICAL: To prepare the 0.1 M NTP stocks, dissolve each powder with RNase-free water. Dissolved NTPs at high concentration will lead to a highly acidic pH. It is critical to adjust the pH of these stock solutions to ~7 using NaOH prior to using them in the transcription reaction.

Note: The use of pyrophosphatase is not required but its presence increases the RNA yield. Strong white precipitation occurs during in vitro transcription in the absence of pyrophosphatase resulting from the insoluble magnesium pyrophosphate side product.

Note: It is recommended to optimize the incubation time of the in vitro transcription for each desired RNA. The transcription reaction can also be performed for 16 h but care should be taken to avoid excessive RNA degradation by contaminating RNases.

16. Quench the in vitro transcription reaction by adding 5 mL of formamide to the 5 mL transcription reaction. If precipitation occurred during the transcription reaction, add 0.5 mL of 0.5 M ethylenediaminetetraacetic (EDTA) to chelate Mg^{2+} and dissolve the magnesium pyrophosphate. Centrifuge briefly to pellet any insoluble material.

Pause point: The quenched transcription mixture can be stored at −20°C or −80°C until purification.

17. Purify the transcripts by preparative denaturing Urea-PAGE as follows:
    a. Prepare the denaturing gel solution by mixing 240 g of urea, 125 mL of 40% polyacrylamide (29:1 acrylamide:bisacrylamide), 50 mL of 10× TBE buffer and add RNase-free water to reach a total volume of 500 mL.
    b. Assemble two glass plates (one notched; the other square) and insert 3 mm thick spacers between them. Hold the assembly together with multiple paper clips while ensuring good contacts between spacers to prevent gel leaks. To help dissipate heat, affix a metal plate with a temperature-reporting sticker behind the glass plates and use desktop fans to cool.
    c. Add 300 μL of N,N,N′,N′-tetramethylethylenediamine (TEMED) and 400 μL of 30% w/v ammonium persulfate (APS) to 300 mL of the gel solution to catalyze polymerization.
    d. Pour the mixture between the glass plates and insert a comb with one or three teeth to form gel-loading wells, depending on the volume of transcription reaction.
    e. Wait at least 1 h for the gel to completely polymerize and solidify.
    f. Fill both upper and lower chambers of the gel assembly with 1× TBE buffer.
    g. Slowly load the quenched transcription mixture into the well using a syringe.
    h. Load into a sub-well on the side of the main well(s) ∼10 μL of denaturing gel loading buffer. This will help track the progression of electrophoresis and also act as markers for RNA size estimation. In addition, an RNA ladder can be loaded but is not required.
    i. Place a desktop fan behind the gel assembly to cool down the system or perform the electrophoresis at 4°C in a cold room.
    j. Run the electrophoresis at 100 W for 4 h, or until the bromophenol blue dye reaches the bottom.

⚠ CRITICAL: Acrylamide and bisacrylamide are neurotoxins when in solution and should be handled with gloves.

⚠ CRITICAL: Avoid air bubbles while pouring the gel solution since this will interfere with the distribution of the electric current during the electrophoresis.

⚠ CRITICAL: The temperature of the glass plates will increase during the electrophoresis and can lead to their breakage. If maintaining the temperature of the plates <50°C is not possible, the electrophoresis settings have to be reduced by lowering the power and increasing the duration.

Note: Wash the well extensively with 1× TBE prior to loading the sample to remove any partially solidified gel pieces, skins or particles.

18. Recover the gel pieces containing the desired RNA: open the gel assembly by prying open the two glass plates with a plastic wedge. Wrap both sides of the gel with saran wrap and place it on top of a silica-coated thin-layer chromatography (TLC) plate. Others have reported using white paper sheets or nylon membranes in place of the TLC plates. Use a hand-held UV lamp to visualize the RNA band. The RNA band should cast a dark shadow on the TLC plate, allowing the marking of the band with a marker pen. Move the marked gel onto a metal plate backing and excise the bands containing RNA with a clean razor blade. Avoid cutting the gel bands on top of the TLC plate, which will destroy it.

⚠ CRITICAL: Reduce to a minimum the time of UV exposure of the gel since this can induce chemical damage to the RNA (Kladwang et al., 2012).

Pause point: The gel pieces containing the desired RNA can be stored at −20°C or −80°C until further purification.

19. Extract the desired RNA from the gel pieces: Use a Whatman Elutrap electroelution system to elute the RNA from the gel pieces by following the manufacturer's instructions.

Alternatives: Instead of electroelution, the RNA can be extracted by crushing the gel pieces and soaking them in 0.3 M sodium acetate pH 5.2 for 16 h at 4°C several times.

20. Concentrate the RNA sample to a volume of ~2 mL using an Amicon centrifugal filter unit with a Molecular weight cutoff (MWCO) of 3 or 10 kDa.
    a. Wash once with 15 mL of 1 M KCl by concentrating down to ~1.5 mL.
    b. Wash three times with 15 mL of RNase-free water by concentrating down to ~1.5 mL.
    c. Filter the sample with 0.22 μm filter.
    d. Measure the RNA concentration with a spectrophotometer device such as a NanoDrop and store the sample in RNase-free water at −20°C or −80°C.

Note: Avoid storing the RNA sample in a buffer solution since this can promote RNA oligomerization (Bou-Nader and Zhang, 2020; Mutschler et al., 2015; Sun et al., 2007).

21. Confirm the purity of the prepared RNA by running an analytical 8 M urea denaturing PAGE. Repeat step 17 with the following adjustments:
    a. Use 1 mm-thick spacer and smaller glass plates.
    b. Add 30 μL of TEMED and 40 μL of 30% w/v APS to 45 mL of denaturing gel solution and pour between the two plates.
    c. Add the denaturing gel loading buffer directly to the RNA sample.
    d. Run the electrophoresis at 50 W for 1 h.
    e. Soak the gel in water containing ethidium bromide or SYBR Gold and image the gel using a gel imager.

Note: A single RNA band of the expected molecular weight should be observed. If the sample shows heterogeneities, please refer to troubleshooting problem 2 below.

⚠ CRITICAL: The approach described above produces homogeneous unmodified $tRNA^{Lys3}$. To obtain post-transcriptionally modified $tRNA^{Lys3}$ please refer to the following references (Bou-Nader et al., 2019; Tisne et al., 2000).

22. Test RNA refolding conditions: Human $tRNA^{Lys3}$ can be easily refolded using a snap cooling procedure leading to a homogenous monomeric RNA (Figure 3B):
    a. Heat 10–30 μM of RNA in 25 mM Tris-HCl pH 7.5 and 150 mM NaCl at 90°C for 2 min.
    b. Quickly transfer the sample onto ice, allow it to cool down over several minutes, and add 2 mM $MgCl_2$ and incubate for an additional 15 min.
23. Confirm the homogeneity of the refolded RNA by non-denaturing PAGE:
    a. Prepare a non-denaturing gel solution by mixing 10 mL of 40% polyacrylamide (29:1 acrylamide:bisacrylamide), 5 mL of 10× THE, 0.5 mL of 1 M $MgCl_2$ and add 34.5 mL of RNase-free water to reach a final volume of 50 mL.
    b. Add 50 μL of TEMED and 80 μL 30% w/v APS to the mixture to initiate polymerization.
    c. Pour the mixture between the two glass plates separated with 1 mm spacers.
    d. Wait at least 90 min for the gel to completely polymerize.
    e. Fill the electrophoresis chambers with 1× THE buffer supplemented with 10 mM $MgCl_2$.
    f. Add non-denaturing gel loading buffer to the sample and load it in the well.
    g. Run the electrophoresis at 25 W for 90 min and ensure that the temperature of the glass plates does not reach above 30°C.

h. Soak the gel in water containing ethidium bromide or SYBR Gold and image the gel using a gel imager.

Note: A single RNA band should be observed. If the sample shows heterogeneities, please refer to troubleshooting problem 3 below.

Note: Mg^{2+} is critical for RNA folding and stability (Yamagami et al., 2021). To ensure that the concentration of Mg^{2+} remains constant during the electrophoresis a peristaltic pump can be used to cycle and mix the running buffers.

Limited proteolysis to identify minimal HIV-1 MA construct suitable for co-crystallization

Timing: 1–3 days

24. Efforts to co-crystallize tRNA with full-length HIV-1 MA (residues 1–131) were unsuccessful despite the fact that this protein was previously crystallized (Hill et al., 1996). Flexible or disordered protein regions can interfere with crystal formation. Therefore, successful crystallization often relies on removing predicted disordered regions or identifying a stable proteolytic fragment using in situ proteolysis to aid crystal formation (Dong et al., 2007).
25. Perform limited proteolysis of MA with trypsin (Figures 4A and 4B):
    a. Mix 3 μg of MA in a total volume of 20 μL of Gel Filtration Buffer with different ratios of trypsin (see Figure 4A).
    b. Incubate the samples for 30 min at 30°C.
    c. Quench the reaction by adding SDS gel-loading buffer and heating at 90°C for 5 min.
    d. Analyze the denatured samples by SDS-PAGE. Bands with faster migration compared to full-length MA should be observed.
    e. Identify the boundaries of the trypsin-resistant fragment by mass spectrometry. The cleavage occurs at K109.

Note: Other proteases such as chymotrypsin can be also used to identify protein fragments suitable for crystallization, depending on the sequence of the target protein.

Note: Once a proper ratio of trypsin has been identified, a kinetic analysis can be performed by repeating step 25 using a single ratio of trypsin while quenching the proteolysis at different time points (Figure 4B).

26. Visualize the identified boundary on the known HIV-1 MA structure determined by nuclear magnetic resonance (NMR) (PDB 2H3I or 2H3F) (Saad et al., 2006). In the NMR ensemble, it is evident that the C-terminal region (residues 109–131) of MA is highly flexible in solution, rationalizing the accessibility of K109 for cleavage by trypsin (Figure 4C). Moreover, the first six residues 1–6 are also disordered.

Note: These dynamic and disordered regions are frequently detrimental to crystallization.

Note: In the absence of experimental structures, AlphaFold can be used to assess the possible protein structure and potentially identify disordered or flexible regions that can be engineered to promote crystallization (Jumper et al., 2021).

27. Engineer a vector expressing a truncated variant of HIV-1 MA (residues 7–108) that lacks the disordered N and C-termini. This can be achieved by using commercially available site-directed mutagenesis kits and the users should follow the manufacturer's instructions.
28. Express and purify MA^{7-108} by repeating steps 1–10 using the new vector generated in step 27.

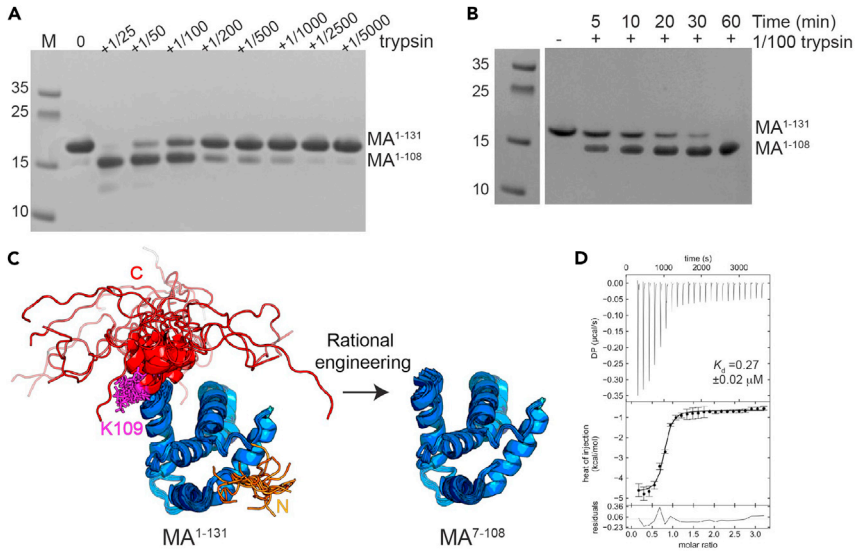

Figure 4. Rational engineering of HIV-1 MA for co-crystallization

(A) Limited proteolysis of MA with different ratio of trypsin.

(B) Kinetics of mild proteolysis of MA with fixed ratio of trypsin.

(C) Visualization of MA flexible and disordered regions (PDB 2H3F). The flexible N-terminus, C-terminus, and the trypsin cleavage site (K109) identified by mass spectrometry are colored in orange, red, and magenta, respectively.

(D) Representative isothermal calorimetry titration of MA with $tRNA^{Lys3}$. Titration was performed in triplicates.

Note: Similar yields are obtained for $MA^{1–131}$ and $MA^{7–108}$.

29. Measure binding of $MA^{1–131}$ and $MA^{7–108}$ to $tRNA^{Lys3}$ by isothermal titration calorimetry (ITC) as follows:
    a. Prepare 350 μM of protein and 30 μM RNA in the Gel Filtration Buffer. This is achieved either by dialyzing the samples for 16 h or by concentrating and diluting the samples in Gel Filtration Buffer at least five times by centrifugation in Amicon filter units.
    b. Load 350 μL of RNA in the cell of the MicroCal iTC200 microcalorimeter.
    c. Load 60 μL of protein in the syringe of the microcalorimeter, avoiding bubble formation and foaming.
    d. Perform the ITC measurement at 25°C while stirring at 750 rpm with a total of 25 injections (1.6 μL of protein injected during each round).

⚠ CRITICAL: $MA^{1–131}$ and $MA^{7–108}$ show similar binding to $tRNA^{Lys3}$ with a dissociation constant K_d of 270 ± 20 nM (Figure 4D). This suggests that the deletions in MA to promote crystallization (1–6 and 109–131) do not interfere with RNA recognition.

Note: If the RNA affinity of the engineered protein is dramatically reduced compared to the wild type, it is likely that the deletions have either directly removed residues located at the recognition interface or indirectly disrupted the interface by compromising protein stability or folding. If attempts to engineer the protein without impacting its RNA affinity fail, the user can skip steps 24–29 and rely on RNA engineering to promote crystallization.

Engineering of human $tRNA^{Lys3}$ to promote crystallization

Timing: 3–7 days

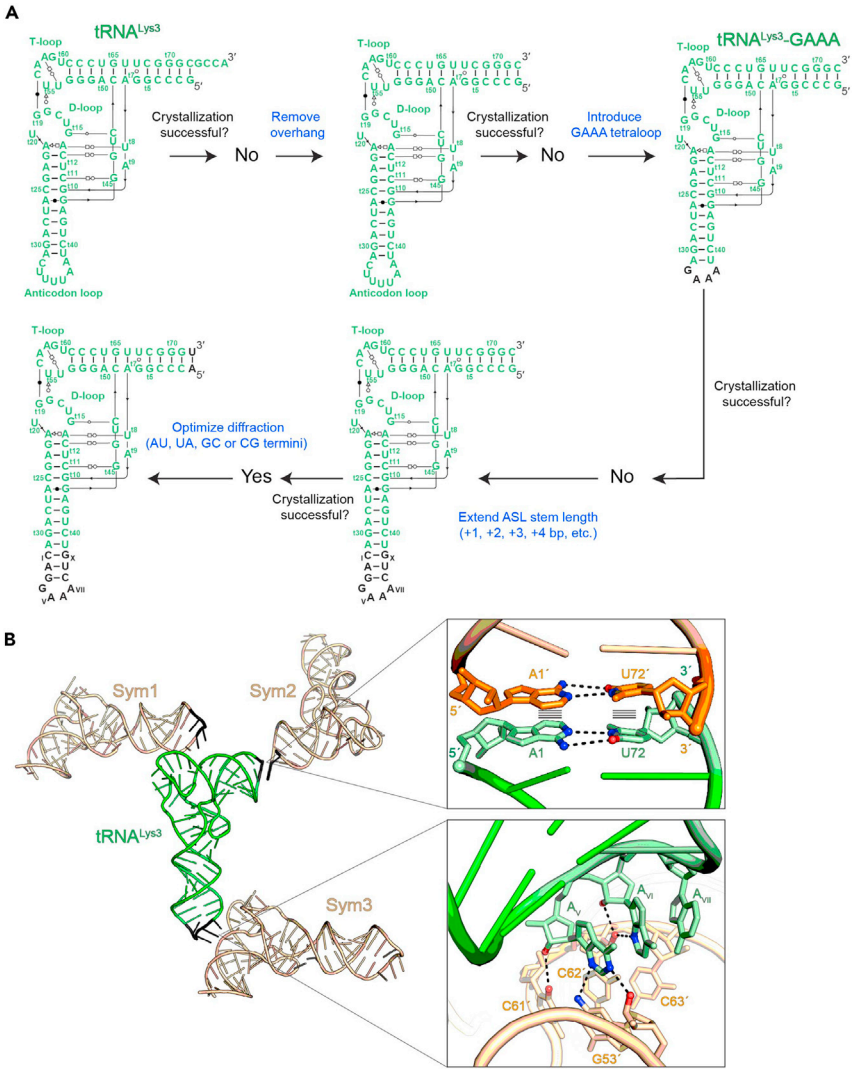

Figure 5. Rational engineering of tRNA^{Lys3} for co-crystallization

(A) Workflow of tRNA^{Lys3} engineering to promote co-crystallization. The natural tRNA sequence is shown in green while the engineered substitutions to enhance crystallization are in black. The 10-nt ASL insertion (in black) is numbered in Roman numerals in order to retain the conventional tRNA numbering in the remaining parts of the tRNA.

(B) Left: Packing arrangement of adjacent tRNA molecules in crystallo. Sym: symmetry-related tRNA molecule. Right: Detailed crystallographic tRNA-tRNA contacts observed at two primary crystal-packing interfaces — between two end-to-end stacked tRNA terminal base pairs and A-minor interactions between the engineered ASL GAAA tetraloop and a dsRNA segment. Hydrogen bonds are shown as dotted lines and stacking interactions as parallel lines. Bound MA is omitted for clarity as it contributes less to the packing than the tRNAs.

30. Efforts to co-crystallize wild type tRNA^{Lys3} with either MA$^{1–131}$ or MA$^{7–108}$ were unsuccessful (Figure 5). The flexible GCCA overhang at the 3′ end of the tRNA can hinder crystallization while co-axial stacking between blunt-ends is a recurrent RNA-RNA contact driving the formation of pseudo-infinite helices frequently seen in crystal structures (Batey et al., 1999; Pujari et al., 2021; Zhang and Ferre-D'Amare, 2014b). To prepare tRNAs lacking the 3′ overhang repeat steps 11–23 while using the following reverse primer 5′-GmCmCCGAACAGGGACTTGAAC-3′ in step 13.
31. To further enhance chances of crystallization, replace the anticodon loop of tRNA^{Lys3} with a GAAA tetraloop. This motif promotes RNA-RNA contacts through A-minor interactions with

neighboring dsRNA and base stacking interactions (using the apex adenosine of the tetraloop) to drive crystal packing (Figure 5B).

a. Substitute the natural anticodon loop sequence CUUUUAA with the GAAA tetraloop in the tRNA gene using commercially available site-directed mutagenesis kits.

b. Repeat steps 11–23 while using the new $tRNA^{Lys3}$ gene containing a GAAA tetraloop ($tRNA^{Lys3}$-GAAA, Figure 5) in step 13.

32. Measure binding of $tRNA^{Lys3}$-GAAA (lacks the 3′ overhang and has the anticodon loop substituted with a GAAA tetraloop) to $MA^{1–131}$ and/or $MA^{7–108}$ by repeating step 29.

Note: Substitution of the anticodon loop with the GAAA tetraloop does not impact binding to MA.

⚠ CRITICAL: Non-conserved regions of the RNA should be typically targeted for engineering. As an alternative, RNA regions not involved in nor impacting the interface being studied can be engineered.

Note: Engineering the tRNA termini is a common approach to promote crystallization, such as extending the stem length or introducing a GAAA tetraloop by circular permutation (Zhang and Ferre-D'Amare, 2013). However, these approaches did not lead to the formation of MA-tRNA co-crystals.

33. Increase the ASL stem length capped by the GAAA tetraloop to sample additional crystallization space and angular orientations for crystal packing.

a. Repeat step 31 while inserting 1 base pair (bp) at a time during site-directed mutagenesis.

Note: Avoid repetition of three or four consecutive guanosines that might lead to inadvertent formation of G-quadruplexes. An ideal sequence to be inserted to extend the ASL has not been systematically tested. It is likely that the length of the stem is the determining factor and different combinations of canonical base pairs can be explored.

b. Test each RNA design for co-crystallization.

Note: A +3-bp insertion above the GAAA tetraloop was necessary to ensure formation of MA-tRNA co-crystals (Figure 5).

34. Since the blunt ends are primarily involved in the crystal packing interface, improve crystal diffraction by testing AU, UA, GC and CG bp at the termini (Figure 5B). We found that an AU terminal bp consistently gave the best diffraction. In the event that diffraction quality cannot be improved further, please refer to troubleshooting problem 4 below.

Note: To prepare the RNA with an A at position 1 in high yields, repeat step 31 while using the following forward primer with a hammerhead ribozyme 5′-GGAATTCCTAATACGACTCAC-TATAGGGAGAGCTATCCGGGTCTGATGAGTCCGTGAGGACGAAACGGTACCCGG-TACCGTCACCCGGATAGCTCAGTCG-3′.

In vitro reconstitution and co-crystallization of HIV-1 MA bound to human $tRNA^{Lys3}$

Timing: 2 days to 1 month

35. To form the ribonucleoprotein complex, mix purified $MA^{7–108}$ and the refolded, engineered $tRNA^{Lys3}$ in a 1.1 : 1 (MA : tRNA) ratio in the Gel Filtration Buffer and incubate at 25°C for 10 min.

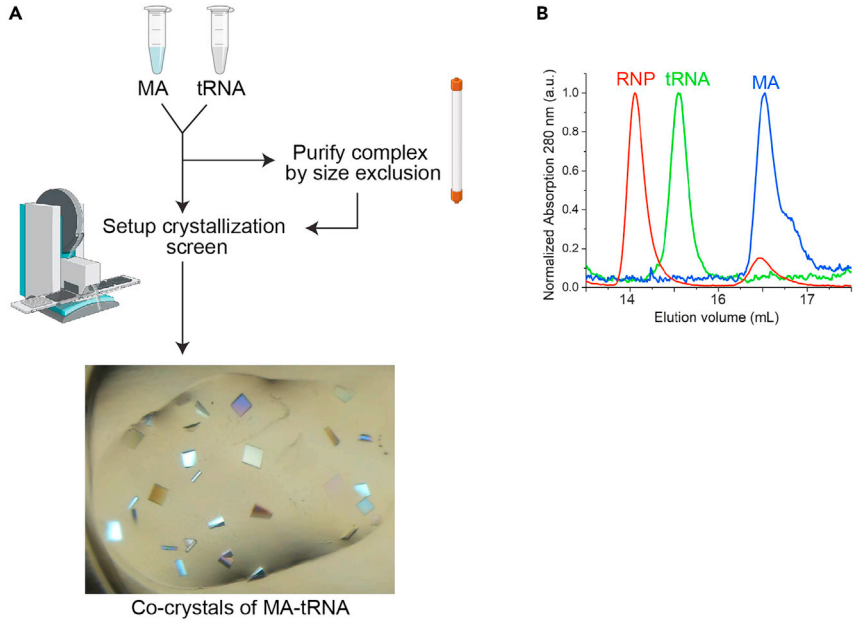

Figure 6. Assembly and purification of MA-tRNA complexes for structural characterization

(A) Workflow to assemble and optionally purify the MA-tRNA complex by size-exclusion chromatography, followed by crystallization trials.

(B) Size-exclusion chromatography profiles of MA, tRNA and the MA-tRNA complex on a Superdex 200 Increase 10/300 GL column.

Note: Mg^{2+} in the buffer not only promotes proper folding and stability of the tRNA but also ensures tighter binding of MA to tRNA.

Note: Different protein:RNA ratios can be tested. Since MA shows robust affinity for tRNA, the addition of an excess amount of protein is not required.

36. Test different commercial crystallization screens using an automated liquid handler for crystal formation (Figure 6A). Mix with a 1:1 ratio the reservoir solution with ~7 mg/mL of freshly reconstituted complex, which contains 593 μM of MA and 540 μM of tRNA.

Note: The crystallization screen can be performed directly with the reconstituted complex or after a size exclusion chromatography purification of the complex to remove any unbound species (Figure 6B). In the context of MA-tRNA, both approaches gave similar results, but this should be systematically tested for each system.

37. Rectangular prism-shaped co-crystals of the dimensions of ~ 50 × 50 × 30 μm^3 are formed with the reservoir solution of 0.1 M HEPES pH 7.5, 20% polyethylene glycol (PEG) 500 monomethyl ether and 10% PEG 20000 at 20°C over 9 days. These crystals are readily reproduced using the hanging-drop and the sitting-drop vapor diffusion methods.

⚠ CRITICAL: While performing crystallization screens for ribonucleoprotein complexes, it is common to obtain crystals containing either one of the components but not both (due to dissociation of the complex during crystallization or efficient crystal packing of only one of the components). To ensure that the crystals contain the complex, their content should be assessed. In the event that co-crystals are not obtained, please refer to troubleshooting problem 5 below.

38. Check crystal content by SDS-PAGE:
    a. Pick 5–8 crystals and wash them at least twice in a stabilizing solution in which crystals do not dissolve (Wash 1 and Wash 2). Usually, the reservoir solution will serve this purpose well. If crystals do dissolve, increase the primary precipitant concentration as needed to prevent crystal dissolution. This washing step is important to remove residual macromolecules adsorbed at the surface of the crystals or present in the liquid during crystal handling. Keep the wash solutions from the washing steps for downstream analysis.
    b. Dissolve washed crystals in RNase-free water. Add ~50 mM EDTA if the crystals do not dissolve readily in water alone.
    c. Add SDS gel loading buffer to the wash 1, wash 2 and the dissolved crystals.
    d. Analyze the three samples by SDS PAGE in addition to two control lanes containing only MA or tRNA as reference markers.
    e. Use Silver Stain to visualize the bands. Commercial or in-house silver stain kits can be used.
    f. Co-crystals should produce two bands on SDS-PAGE by Silver Stain, one attributed to MA and the other to tRNA.

Note: Different commercial silver stain kits stain proteins and RNAs with different efficiencies. As a result, the intensity of the bands might not be proportional to the ratio of proteins and RNAs in the crystal. Nevertheless, if both bands are identified in the dissolved crystals and the band intensities are significantly stronger than those from Wash 1 and Wash 2, then it is reasonable confirmation that the crystals contain both components.

39. Transfer single crystals into a cryo-protection solution containing 0.1 M HEPES pH 7.5, 30% polyethylene glycol (PEG) 500 monomethyl ether and 10% PEG 20000 using cryoloops, which can be obtained from Hampton Research, MiTiGen, etc.
40. Loop individual crystals and vitrify them in liquid nitrogen.

Note: Liquid nitrogen should always be handled with gloves and goggles and in well-ventilated areas.

41. Collect X-ray diffraction data at the synchrotron or on an in-house X-ray source.

Structure determination by molecular replacement and refinement

Timing: 2–5 h

42. Process the collected X-ray diffraction images using a peak-finding, indexing, integration and scaling software (XDS, DIALS, HKL2000, Mosfilm, Xia2, etc). The MA-tRNA co-crystals described in this protocol were indexed in space group *I* 2 2 2 with the following unit cell parameters: a, b, c = 96.72, 108.85, 146.02 Å; α , β, γ = 90, 90, 90°.
43. Perform Molecular Replacement (MR) using Phaser (McCoy et al., 2007) to phase the structure (Figure 7).
    a. Perform a first search looking for two MA molecules in the asymmetric unit. Use as a starting model one molecule of PDB 1HIW with residues 110–121 removed. Searching for MA first and tRNA later is advantageous due to the more rigid MA core, compared to the more flexible tRNA structure.
    b. This first MR solution (solution 1 in Figure 7) shows a Translation Function Z score (TFZ) of 20 and a Log-likelihood Gain (LLG) of 300.8 suggesting the identification of a correct solution.
    c. Perform a second search looking for one tRNA molecule in the asymmetric unit while using preliminary MR phases from solution 1. Use as search model PDB 1FIR with residues 32–38 and 73–76 removed.
    d. This second MR solution (solution 2 in Figure 7) shows a TFZ of 36.5 and LLG of 1216.9.

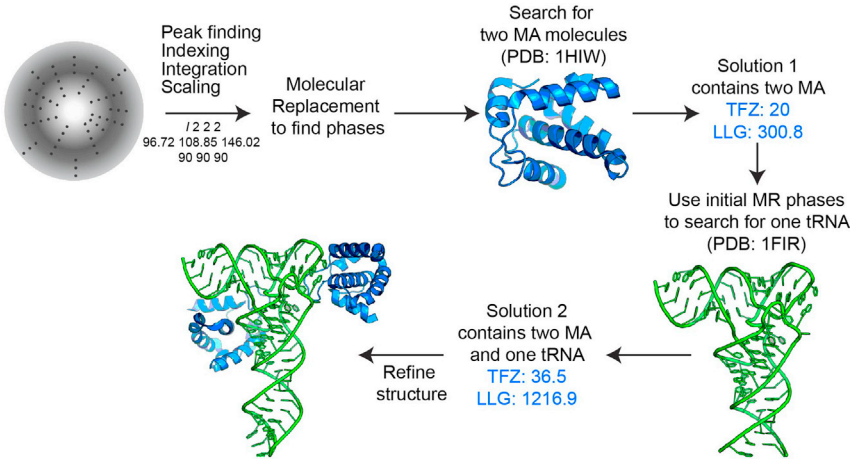

Figure 7. Two-step molecular replacement procedure to solve the co-crystal structure of MA-tRNA complex

⚠ CRITICAL: Searching simultaneously for two MA and one tRNA during MR did not identify the final correct solution. Instead, solutions containing either two MA molecules or only one tRNA molecule are found. It is possible that the lower resolution of the structure (3.15 Å) or conformational deviations between the search model and actual structures hinders the accurate concurrent placement of the three molecules using Phaser.

Note: MR were unsuccessful when using MA models derived from NMR structures such as PDB 2H3F (either using the entire NMR ensemble of 20 conformers or using individual conformers).

44. Refine the initial Phaser-placed structure using Phenix.Refine (Liebschner et al., 2019) and perform iterative rounds of manual model building and adjustments using Coot (Emsley et al., 2010).
45. Optimize the nucleic acid structure using ERRASER (Chou et al., 2013) and repeat step 44.

TROUBLESHOOTING

Problem 1

Significant amount of protein is still present in the supernatant despite the ammonium sulfate precipitation.

Potential solution

Increase the duration of the ammonium sulfate precipitation to 16 h at 4°C.

Problem 2

RNA transcripts exhibit 5′ and/or 3′ heterogeneity.

Potential solution

To ensure 5′ homogeneity, use the hammerhead (HH) ribozyme by changing the forward primer to the following sequence: GGAATTCCTAATACGACTCACTATA*GGGAGA***GCTATCCGGGC***CTGATGAGTC CGTGAGGACGAAACGGTACCCGGTACCGTC*GCCCGGATAGCTCAGTCGGT.

Underlined is the T7 promoter sequence, in italic is the HH 5′ nucleotides, in bold is the 11-nt reverse complement of the 5′ region of the desired transcript and in italic and underlined is the HH 3′ nucleotides. HH self-cleavage occurs co-transcriptionally with >80% efficiency and leaves a 5′-hydroxyl on the 3′ desired RNA.

To ensure 3′ homogeneity, use the Varkud Satellite (VS) ribozyme (Suslov et al., 2015) by changing the reverse primer to the following sequence: UmCmGGGGCGACGACGCCCTTTGGCGCC CGAACAGGGACTTGAACCC.

In bold is the reverse complement of the VS substrate and underlined are the 2′-O-methyl-modified nucleotides. The VS ribozyme is prepared separately and added in trans to the desired transcripts. It is recommended to optimize the cleavage efficiency and RNA yield by testing different ratios of DNA template, VS ribozyme as well as incubation times. The trans cleavage by the VS ribozyme leaves a 2′,3′-cyclic phosphate at the 3′ end of the desired RNA. To open this cyclic phosphate, the transcripts can be treated with 10 mM HCl at 4°C for 30 min yielding a regular 3′ phosphate (Li et al., 2019; Xiao et al., 2008).

Problem 3

Multiple RNA bands are observed by non-denaturing PAGE while a single RNA band is detected by denaturing PAGE. This suggests misfolding, conformational heterogeneity or oligomerization of the RNA during the refolding procedure. Many complex RNAs easily misfold, such as full-length T-box riboswitches in the absence of their tRNA ligands (Li et al., 2019).

Potential solution

Modify the buffer conditions of refolding by replacing NaCl with KCl or increasing the concentration of $MgCl_2$ to 10–20 mM. In addition, other refolding procedures can be attempted such as a slow cooling (annealing) protocol:

PCR cycling conditions

Steps	Temperature	Time	Cycles
Denaturation	90°C	3 min	1
Slow cooling	89°C (−1°C increment per cycle)	30 s	23 cycles
Pause Point	65°C	forever	
Add $MgCl_2$			
Slow cooling	64°C (−1°C increment per cycle)	30 s	42 cycles
Hold	4°C	forever	

While most tRNAs and other relatively simple structured RNAs such as the Adenovirus VA-I RNA refold readily after denaturing purification (Dupasquier et al., 2008; Hood et al., 2019; Westhof and Auffinger, 2001), many complex RNAs do not properly refold once denatured (Batey and Kieft, 2007). For these RNAs, native purification is recommended, such as in the case of several T-box riboswitch domains (Li et al., 2019). Native RNA purification can be accomplished by either preparative non-denaturing PAGE (without Urea), size-exclusion chromatography or anion-exchange chromatography, or using several ribozyme-cleavable affinity tags (Batey and Kieft, 2007; Easton et al., 2010; Li et al., 2019; Suddala and Zhang, 2019).

Problem 4

Co-crystals are obtained but show limited resolution and additional engineering of the RNA does not improve diffraction quality.

Potential solution

An alternative to improving crystal diffraction is post-crystallization treatments (Heras and Martin, 2005; Reyes et al., 2009; Zhang and Ferre-D'Amare, 2014a). Dehydration, soaking, cation replacement and annealing of crystals are all approaches that should be tested to improve the diffraction quality (Zhang and Ferre-D'Amare, 2015).

Problem 5

Co-crystals are not obtained while crystals of free MA or free tRNA are formed.

Potential solution

Test if the RNA is degraded during the crystallization process. Since most crystallization events span a few days and weeks, trace amounts of contaminating RNases in the protein preparation can degrade the RNA and hinder co-crystallization. Each batch of purified protein should be tested for residual RNase activity. This can be done using commercially available kits or simply by incubating the protein and RNA at several time points (1 h, 2 h, 5 h, 24 h, 48 h, 72 h, etc.) at 25°C and checking the integrity of the RNA by denaturing PAGE described in step 21.

RESOURCE AVAILABILITY

Lead contact

Further information and requests for resources and reagents should be directed to and will be fulfilled by the lead contact, Jinwei Zhang (jinwei.zhang@nih.gov).

Materials availability

This study did not generate new unique reagents.

Data and code availability

Atomic coordinates and structure factor amplitudes for $tRNA^{Lys3}$ bound to HIV-1 MA have been deposited in the Protein Data Bank (PDB) under accession code 7MRL.

This study did not generate any original code.

Any additional information required to reanalyze the data reported in this paper is available from the lead contact upon request.

ACKNOWLEDGMENTS

We thank I. Botos for computational support, G. Piszczek, D. Wu for support in biophysical analyses, Y. He and N. Tjandra for fermentation support, R. Levine and D.-Y. Lee for mass spectrometry support, and J.L. Smith and K. Suddala for discussions. Some figures were created with https://biorender.com. X-ray diffraction data were collected at SER-CAT 22-ID beamline at the Advanced Photon Source of the Argonne National Laboratory, supported by the U. S. Department of Energy under Contract No. W-31-109-Eng-38. This work was supported by the Intramural Research Program of the NIH, The National Institute of Diabetes and Digestive and Kidney Diseases (NIDDK) (ZIADK075136 to J.Z.), and a NIH Deputy Director for Intramural Research (DDIR) Challenge Award to J.Z. C.B.N. is a recipient of an NIH Intramural AIDS Research Fellowship and an NIDDK Nancy Nossal Fellowship Award.

AUTHOR CONTRIBUTIONS

C.B.N. drafted the manuscript and prepared figures. J.Z. edited the manuscript.

DECLARATION OF INTERESTS

The authors declare no conflict of interests.

REFERENCES

Batey, R.T., and Kieft, J.S. (2007). Improved native affinity purification of RNA. RNA *13*, 1384–1389.

Batey, R.T., Rambo, R.P., and Doudna, J.A. (1999). Tertiary Motifs in RNA structure and folding. Angew. Chem. Int. Ed. Engl. *38*, 2326–2343.

Bou-Nader, C., Barraud, P., Pecqueur, L., Perez, J., Velours, C., Shepard, W., Fontecave, M., Tisne, C., and Hamdane, D. (2019). Molecular basis for transfer RNA recognition by the double-stranded RNA-binding domain of human dihydrouridine synthase 2. Nucleic Acids Res. *47*, 3117–3126.

Bou-Nader, C., Muecksch, F., Brown, J.B., Gordon, J.M., York, A., Peng, C., Ghirlando, R., Summers, M.F., Bieniasz, P.D., and Zhang, J. (2021). HIV-1 matrix-tRNA complex structure reveals basis for host control of Gag localization. Cell Host Microbe *29*, 1421–1436.e1427.

Bou-Nader, C., and Zhang, J. (2020). Structural insights into RNA dimerization: motifs, interfaces and functions. Molecules *25*, 2881.

Burgess, R.R. (2009). Chapter 20 protein precipitation techniques. In Guide to Protein Purification, 2nd Edition, pp. 331–342.

Chou, F.C., Sripakdeevong, P., Dibrov, S.M., Hermann, T., and Das, R. (2013). Correcting pervasive errors in RNA crystallography through enumerative structure prediction. Nat. Methods *10*, 74–76.

Cole, J.L., Lary, J.W., Moody, T., and Laue, T.M. (2008). Analytical ultracentrifugation: sedimentation velocity and sedimentation equilibrium. In Biophysical Tools for Biologists, Volume One: In Vitro Techniques, pp. 143–179.

Dong, A., Xu, X., Edwards, A.M., Midwest Center for Structural Genomics; Structural Genomics Consortium, Chang, C., Chruszcz, M., Cuff, M., Cymborowski, M., Di Leo, R., et al. (2007). In situ proteolysis for protein crystallization and structure determination. Nat. Methods *4*, 1019–1021.

Dupasquier, M., Kim, S., Halkidis, K., Gamper, H., and Hou, Y.M. (2008). tRNA integrity is a prerequisite for rapid CCA addition: implication for quality control. J. Mol. Biol. *379*, 579–588.

Easton, L.E., Shibata, Y., and Lukavsky, P.J. (2010). Rapid, nondenaturing RNA purification using weak anion-exchange fast performance liquid chromatography. RNA *16*, 647–653.

Emsley, P., Lohkamp, B., Scott, W.G., and Cowtan, K. (2010). Features and development of Coot. Acta Crystallogr. D Biol. Crystallogr. *66*, 486–501.

Ferré-D'Amaré, A.R., and Doudna, J.A. (1996). Use of cis- and trans-ribozymes to remove 5′ and 3′ heterogeneities from milligrams of in vitro transcribed RNA. Nucleic Acids Res. *24*, 977–978.

Gaines, C.R., Tkacik, E., Rivera-Oven, A., Somani, P., Achimovich, A., Alabi, T., Zhu, A., Getachew, N., Yang, A.L., McDonough, M., et al. (2018). HIV-1 matrix protein interactions with tRNA: implications for membrane targeting. J. Mol. Biol. *430*, 2113–2127.

Heras, B., and Martin, J.L. (2005). Post-crystallization treatments for improving diffraction quality of protein crystals. Acta Crystallogr. D Biol. Crystallogr. *61*, 1173–1180.

Hill, C.P., Worthylake, D., Bancroft, D.P., Christensen, A.M., and Sundquist, W.I. (1996). Crystal structures of the trimeric human immunodeficiency virus type 1 matrix protein: implications for membrane association and assembly. Proc. Natl. Acad. Sci. U S A. *93*, 3099–3104.

Hood, I.V., Gordon, J.M., Bou-Nader, C., Henderson, F.E., Bahmanjah, S., and Zhang, J. (2019). Crystal structure of an adenovirus virus-associated RNA. Nat. Commun. *10*, 2871.

Jumper, J., Evans, R., Pritzel, A., Green, T., Figurnov, M., Ronneberger, O., Tunyasuvunakool, K., Bates, R., Zidek, A., Potapenko, A., et al. (2021). Highly accurate protein structure prediction with AlphaFold. Nature *596*, 583–589.

Kao, C., Zheng, M., and Rudisser, S. (1999). A simple and efficient method to reduce nontemplated nucleotide addition at the 3 terminus of RNAs transcribed by T7 RNA polymerase. RNA *5*, 1268–1272.

Keller, S., Vargas, C., Zhao, H., Piszczek, G., Brautigam, C.A., and Schuck, P. (2012). High-precision isothermal titration calorimetry with automated peak-shape analysis. Anal Chem. *84*, 5066–5073.

Kladwang, W., Hum, J., and Das, R. (2012). Ultraviolet shadowing of RNA can cause significant chemical damage in seconds. Sci. Rep. *2*, 517.

Li, S., Su, Z., Lehmann, J., Stamatopoulou, V., Giarimoglou, N., Henderson, F.E., Fan, L., Pintilie, G.D., Zhang, K., Chen, M., et al. (2019). Structural basis of amino acid surveillance by higher-order tRNA-mRNA interactions. Nat. Struct. Mol. Biol. *26*, 1094–1105.

Liebschner, D., Afonine, P.V., Baker, M.L., Bunkoczi, G., Chen, V.B., Croll, T.I., Hintze, B., Hung, L.W., Jain, S., McCoy, A.J., et al. (2019). Macromolecular structure determination using X-rays, neutrons and electrons: recent developments in Phenix. Acta Crystallogr. D Struct. Biol. *75*, 861–877.

McCoy, A.J., Grosse-Kunstleve, R.W., Adams, P.D., Winn, M.D., Storoni, L.C., and Read, R.J. (2007). Phaser crystallographic software. J. Appl. Crystallogr. *40*, 658–674.

Mutschler, H., Wochner, A., and Holliger, P. (2015). Freeze-thaw cycles as drivers of complex ribozyme assembly. Nat. Chem. *7*, 502–508.

Pujari, N., Saundh, S.L., Acquah, F.A., Mooers, B.H.M., Ferré-D'Amaré, A.R., and Leung, A.K.-W. (2021). Engineering crystal packing in RNA structures I: past and future strategies for engineering RNA packing in crystals. Crystals *11*, 952.

Reyes, F.E., Garst, A.D., and Batey, R.T. (2009). Strategies in RNA crystallography. In Biophysical, Chemical, and Functional Probes of RNA Structure, Interactions and Folding: Part B, pp. 119–139.

Saad, J.S., Miller, J., Tai, J., Kim, A., Ghanam, R.H., and Summers, M.F. (2006). Structural basis for targeting HIV-1 Gag proteins to the plasma membrane for virus assembly. Proc. Natl. Acad. Sci. U S A. *103*, 11364–11369.

Schuck, P. (2000). Size-distribution analysis of macromolecules by sedimentation velocity ultracentrifugation and lamm equation modeling. Biophys. J. *78*, 1606–1619.

Suddala, K.C., and Zhang, J. (2019). High-affinity recognition of specific tRNAs by an mRNA anticodon-binding groove. Nat. Struct. Mol. Biol. *26*, 1114–1122.

Sun, X., Li, J.M., and Wartell, R.M. (2007). Conversion of stable RNA hairpin to a metastable dimer in frozen solution. RNA *13*, 2277–2286.

Suslov, N.B., DasGupta, S., Huang, H., Fuller, J.R., Lilley, D.M., Rice, P.A., and Piccirilli, J.A. (2015). Crystal structure of the Varkud satellite ribozyme. Nat. Chem. Biol. *11*, 840–846.

Tang, C., Loeliger, E., Luncsford, P., Kinde, I., Beckett, D., and Summers, M.F. (2004). Entropic switch regulates myristate exposure in the HIV-1 matrix protein. Proc. Natl. Acad. Sci. U S A. *101*, 517–522.

Tisne, C., Rigourd, M., Marquet, R., Ehresmann, C., and Dardel, F. (2000). NMR and biochemical characterization of recombinant human tRNA(Lys)3 expressed in Escherichia coli: identification of posttranscriptional nucleotide modifications required for efficient initiation of HIV-1 reverse transcription. RNA *6*, 1403–1412.

Westhof, E., and Auffinger, P. (2001). Transfer RNA Structure (eLS).

Xiao, H., Murakami, H., Suga, H., and Ferré-D'Amaré, A.R. (2008). Structural basis of specific tRNA aminoacylation by a small *in vitro* selected ribozyme. Nature *454*, 358–361.

Yamagami, R., Sieg, J.P., and Bevilacqua, P.C. (2021). Functional roles of chelated magnesium ions in RNA folding and function. Biochemistry *60*, 2374–2386.

Zhang, J., and Ferre-D'Amare, A.R. (2013). Co-crystal structure of a T-box riboswitch stem I domain in complex with its cognate tRNA. Nature *500*, 363–366.

Zhang, J., and Ferre-D'Amare, A.R. (2014a). Dramatic improvement of crystals of large RNAs by cation replacement and dehydration. Structure *22*, 1363–1371.

Zhang, J., and Ferre-D'Amare, A.R. (2014b). New molecular engineering approaches for crystallographic studies of large RNAs. Curr. Opin. Struct. Biol. *26*, 9–15.

Zhang, J., and Ferre-D'Amare, A.R. (2015). Post-crystallization improvement of RNA crystals by synergistic ion exchange and dehydration. Bio Protoc. *5*, e1578.

Zhao, H., Ghirlando, R., Piszczek, G., Curth, U., Brautigam, C.A., and Schuck, P. (2013). Recorded scan times can limit the accuracy of sedimentation coefficients in analytical ultracentrifugation. Anal Biochem. *437*, 104–108.

Zhao, H., Piszczek, G., and Schuck, P. (2015). SEDPHAT–a platform for global ITC analysis and global multi-method analysis of molecular interactions. Methods *76*, 137–148.